MODELLING AND CONTROL OF MOBILE ROBOTS

Bashir M. Y. Nouri

The Hashemite University
Department of Mechatronics Engineering
P. O. Box 150459, Zarqa 13115, Jordan.
bnouri@hu.edu.jo or bashir_nouri@yahoo.com

ABSTRACT

Mobile robots is a relatively new research area that is normally considered from several different perspectives mainly, engineering and computer science levels. This paper deals with the engineering level of mobile platforms; i.e. the physical, hardware and mechatronic levels of mobile platforms, and presents complete models for the main hardware components of mobile platforms. The presented models can be used for simulation and control of mobile platforms, and they take into account the hardware limitations, friction force and the topography of the environment for out door navigation.

1. INTRODUCTION

Mobile robotics is a relatively new research area that deals with control of autonomous and semiautonomous vehicles. Mobile robots can be considered from several different perspectives: Firstly, physical, hardware, and mechatronic levels; i.e. engineering level, secondly, software level; i.e. computer science level, [1]. Most the research done on mobile robots focused on the software level and concentrated on programming autonomous mobile robots for performing tasks; such as, path following, see e.g. [2] and [3], obstacle avoidance, see e.g. [4], navigation in known or unknown environments, etc. Most the previous research considered the geometric modeling of mobile robots. Unlike physical, hardware and mechatronic modeling, geometric modeling includes scaling, rotation, translation, and geometry representation [5]. Few research is done on the physical, hardware and mechatronic levels of mobile robots, where robots can be decomposed into: First, a mechanism for making the robot move through its environment; the physical organization of motors, belts, and gears necessary to make the robot move. Second, a computer or a collection of computers for controlling the robot. Third, a collection of sensors with which the robot gathers information concerning its environment. Four, communications hardware to enable the robot to communicate to an off-board operator and any externally based computers; typical examples include serial or Ethernet connections (both wireless and direct).

Most the done research on mobile robots considers the software point of view and the geometric modeling of mobile platforms, and did not consider the limitations of the hardware; such as, the limitations of the dc motors that normally drive mobile robots (currents, voltages, torques, and velocities), the inertia of robot, the friction force between mating surfaces, and the topography of the environment for out door navigation. This paper presents a complete physical model on the mechatronic level of wheeled mobile robots. The model can be used to simulate different wheeled mobile platforms based on the available information about the main components constructing the robot (see Figure 1); such as, the data sheets of dc motors, the wheels, the sensors, etc. The models can be used for designing and building mobile robots. The model also helps the researchers who consider the software point of view of mobile robots to take into account the limitations of the hardware of mobile robots, instead of considering only the external dimensions of the robots or the geometric model.

Figure 1 presents a sketch of a general three-wheels mobile robot showing all the considered hardware components of the robot. Section 2 presents a physical model of the power actuator devices (DC motors) that normally deliver energy to the rear wheels of a mobile robot, note that the front wheel is a caster wheel. Section 3 completes the model of a servo dc motor by modeling a tacho-generator that is normally used to measure that velocity of the robot and indirectly the location (by integrating the measured velocity) of the robot in its environment. Section 4 models the topography as external disturbance acting on the actuator devices of the robot. Section 5 presents an analogue velocity controller for the servomotors of the robot, and a global simulation model for the considered mobile robot. Section 6 concludes the paper with some comments.

2. MODELLING THE POWER ACTUATOR DRIVE

Usually, mobile platforms are supported by two driving wheels (e.g. rear wheels); and with stability augmented by one or two front caster wheel(s); see Figure 1. Direct current (DC) motors that are coupled directly or indirectly (via velocity reduction gears) with the driving wheels are

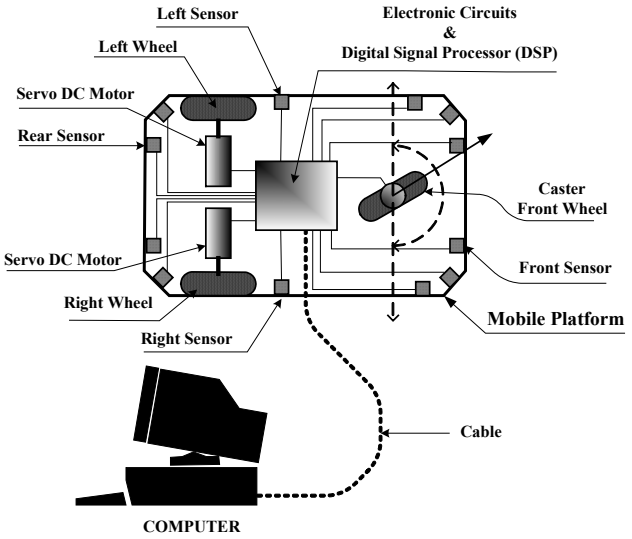

Figure 1. *Sketch of a general three-wheels mobile platform showing the main hardware components.*

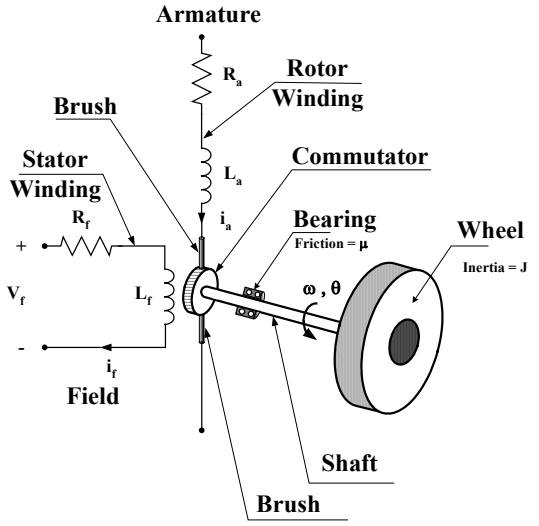

Figure 2. *Circuit diagram of a power actuator drive of a general mobile platform.*

usually used to actuate mobile platforms because their torque-speed characteristics are achievable with different electrical configurations and their speeds can be smoothly controlled and in most cases are reversible. This section presents a complete physical model and identifies the whole parameters of a DC motor coupled directly to a driving wheel. Figure 2 shows a circuit diagram of a power actuator drive of a general mobile platform. A dc motor consists of two main components: stator winding and rotor winding. These components have the function of converting electrical energy to mechanical energy. DC motors can be classified into two categories: Firstly, armature controlled dc motors where the field voltage (V_f) is held constant, or a permanent magnate replaces the stator winding. They are controlled by varying the armature voltage (V_a) or current (i_a). Secondly, Field controlled dc motors where the armature voltage (V_a) is held constant and controlled by varying the field voltage (V_f) or current (i_f).

In modelling dc motors and in order to obtain a linear model, the hysteresis and the voltage drop across the motor brushes is neglected, and the motor input voltage may be applied to the field or armature terminals [6].
The air gap flux (ϕ) is proportional to the field current (i_f) as follows:

$$\phi = K_f\, i_f(t) \qquad (1)$$

where K_f is the proportionality constant and t is time.
The torque (T_m) developed by the motor is assumed to be related linearly (K_1 is the proportionality constant) to ϕ and the armature current (i_a), and substituting for air gap flux(ϕ) from Equation 1 yields:

$$T_m(t) = K_1\, \phi\, i_a(t) = K_1 K_f\, i_f(t)\, i_a(t) \qquad (2)$$

Equation 2 shows that to have a linear dc motor, one current (i_f or i_a) must be maintained constant while the other current becomes the input current controlled motor.

Case 1: Field current controlled DC motor

In the field current controlled dc motors, the armature current (i_a) is held constant and the field current (i_f) varies with time (t) yields:

$$T_m(t) = K_1\, \phi\, i_a = (K_1 K_f\, i_a)\, i_f(t) = K_m\, i_f(t) \qquad (3)$$

Where: ($K_m = K_1 K_f i_a$) is called the dc motor constant.
Applying Kirchhoff's voltage law to the stator (field) of the dc motor, and using Laplace notation yields:

$$V_f(s) = (R_f + L_f\, s)\, I_f(s) \qquad (4)$$

Where: s is the Laplace operator, V_f is the stator input voltage, R_f is the stator resistance, L_f is the stator inductance, and $I_f = i_f$ is the stator current, see Figure 2.
The motor torque (Equation 3) equals the torque delivered to the wheel and rotor (T_R) that can be modeled by:

$$T_R(s) = J s^2\, \theta(s) + \mu\, s\, \theta(s) \qquad (5)$$

Where: T_R is the torque delivered to the wheel, J is the inertia of the wheel and the rotor of the dc motor, μ is the viscous friction coefficient between the rotor shaft and the bearings of the dc motor, and $\dot{\theta}$ and $\ddot{\theta}$ are the angular velocity and angular acceleration of the wheel, respectively.
Equating Equation 3 (after rewriting it in Laplace notation) with Equation 5, and substituting for $I_f(s)$ from Equation 4 yields the transfer function, G(s), of a field current controlled dc motor connected directly to a wheel:

$$G(s) = \frac{\theta(s)}{V_f(s)} = \frac{K}{s(\tau_f\, s + 1)(\tau_R\, s + 1)} \qquad (6)$$

with $K = \dfrac{K_m}{\mu R_f} = \dfrac{K_1 K_f I_a}{\mu R_f}$, $\tau_f = \dfrac{L_f}{R_f}$ and $\tau_R = \dfrac{J}{\mu}$

Where: K is the system fixed gain, τ_f is the stator (field) time constant (electrical time constant), and τ_R is the rotor

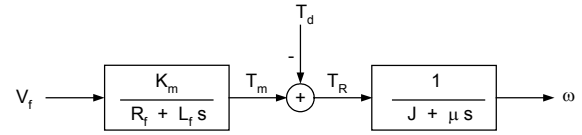

Figure 3. *Block diagram of a field control power actuator drive of a general mobile robot.*

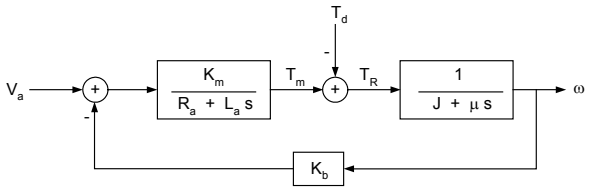

Figure 4. *Block diagram of armature control power actuator drive of a general mobile robot.*

and wheel time constant (mechanical time constant).
Figure 3 presents a block diagram of a field control power actuator drive of a general mobile robot that is suitable for simulation and control with the aid of computer simulation package, e.g. SIMULINK software. Note that T_m is the generated mechanical torque of the motor, see Equation 3, T_d is the disturbing torque, see later section 4, T_R is the driving torque of the motor's rotor and the wheel, see Equation 5, and ω is the wheel's angular velocity.

Case 2: Armature controlled DC motor

In armature controlled dc motors, the field current (i_f) is constant or the stator winding is replaced by a permanent magnate and the armature current (i_a) varies with time (t) yields:

$$T_m(t) = K_1 \phi i_a = (K_1 K_f i_f)\, i_a(t) = K_m i_a(t) \qquad (7)$$

Where: ($K_m = K_1 K_f i_f$) is called the dc motor constant.
Applying Kirchhoff's voltage law to the rotor (armature) of the dc motor and using Laplace notation yields:

$$V_a(s) = (R_a + L_a s) I_a(s) + V_b(s) \qquad (8)$$

Where: V_a is the armature input voltage, V_b is the back electromotive-force voltage proportional to the motor speed $\left(V_b(t) = K_b \omega(t)\right)$, and R_a , L_a and I_a are the armature resistance, inductance, and current, respectively (see Figure 2). Equating Equation 7 (after rewriting it using La place notation, and substituting for $I_a(s)$ from Equation 8) with Equation 5, and rearranging yields the transfer function, G(s), of an armature current controlled dc motor connected directly to a wheel:

$$G(s) = \frac{\theta(s)}{V_a(s)} = \frac{K_m}{s\left[(R_a + L_a s)(Js + \mu) + K_b K_m\right]} \qquad (9)$$

Figure 4 presents a block diagram of armature control power actuator drive of a general mobile robot that is suitable for simulation and control with the aid of computer simulation package, e.g. SIMULINK software. Note that T_m is the generated mechanical torque of the motor, see Equation 7, T_d is the disturbing torque, see later section 4, T_R is the driving torque of the motor's rotor and the wheel, see Equations 5, and ω is the wheel's angular velocity.

3. MODELLING THE VELOCITY SENSOR

A servo dc motor usually consists of a dc motor and a velocity sensor, e.g. a tachogenerator (a tachometer) where the measured angular velocity is proportional to the output voltage of the meter; or an incremental encoder where the measured angular velocity is proportional to the counted increments in a known period of time. This section models a tachometer (generator) and completes the model of a servo dc motor. Figure 5 presents the circuit diagram that normally used to analyse tachogenerator or tachometer velocity sensors. It consists of a rotor that is coupled directly to the shaft of the driving dc motor, and a stator winding; i.e. the tachometer or tachogenerator velocity sensor can be considered as a reversed permanent magnet dc motor (dc generator).
The internal generated voltage (U_r) in the tachometer is given by:

$$U_r = K \omega \qquad (10)$$

Where: U_r is the internal generated voltage of a tachogenerator (volts) that is equivalent to the back e.m.f. of a dc motor. K is the proportionality constant (volts . second / radians) and ω is the input angular speed (rad/ s).

Applying Kirchhoff's voltage law to the rotor (armature) of the tachogenerator yields:

$$U_r = L\frac{di}{dt} + R i + U \qquad (11)$$

Where U is the output terminal voltage. L is the inductance and R is the resistance of the armature winding of the generator.

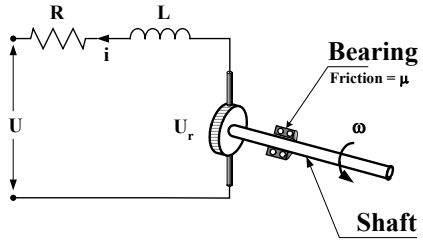

Figure 5. *Circuit diagram of a tachogenerator or tachometer velocity sensor.*

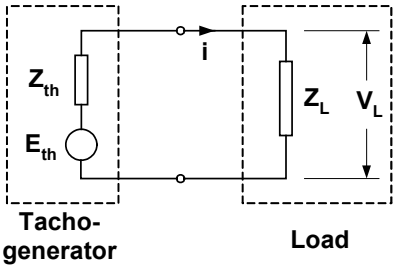

Figure 6. *Equivalent Thévinen circuit of a Loaded tachogenerator or tachometer velocity sensor.*

It is clear from Equation 11 the existence of a measurement error (losses in the impedance of the generator). This error can easily and significantly reduced by loading the velocity sensor; see e.g. [7], as follows:

Consider the equivalent Thévinen circuit of the sensor (Figure 6) where U_r is equivalent to Thévinen voltage (E_{th}), (Ls + R) is equivalent to Thévinen impedance (Z_{th}) and Z_L is the impedance of the load such as recorder or signal conditioning element, e.g. comparator that normally used in designing analog control circuits that are necessary in velocity control of dc motors, and V_L is equivalent to U. The voltage V_L across the load is given by:

$$V_L = \frac{Z_L}{Z_{th} + Z_L} E_{th} \tag{12}$$

If Z_L represents the input impedance of a comparator that is very large and much greater than the impedance of the tachogenerator (represented by Z_{th}), then V_L becomes approximately equal E_{th}, and $U = U_r$ yields:

$$U = K\,\omega \tag{13}$$

and the transfer function of the tachogenerator becomes:

$$G_{Tacho}(s) = \frac{U(s)}{\omega(s)} = K \tag{14}$$

Where K is the conversion gain, i.e. a specific-fixed value for a given tachogenerator or tachometer angular velocity sensor.

4. MODELLING THE TOPOGRAPHY

The surface of the topography acts by two ways as an external disturbance on the actuator drives of wheeled mobile robots: Firstly, the changes in the inclination angle (β) of the topography causes the weight component (F_w) of the robot to act positively, i.e. added to the driving force (F_d), or negatively, i.e. subtracted from the driving force (F_d). Secondly, the friction (F_f) between the wheels and the surface of the topography of contact acts negatively, i.e. subtracted from the driving force (F_d) of the actuator drives, see Figure 7.

Reading Figure 7 and summing up the forces yields:

$$F_d = F_i + F_w + F_f \tag{15}$$

and $$F_d = M_r\,\ddot{x} + M_r\,g\sin(\beta) + F_f$$

where: F_d is the total driving force applied by the two actuator drives, F_i is the total inertia force of the mobile platform, F_w is the total weight component of the robot, and F_f is the total friction force between the wheels and

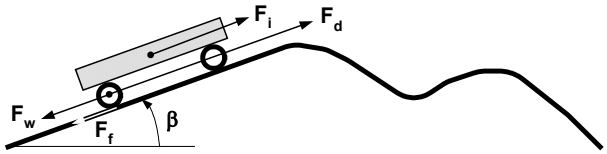

Figure 7. *Disturbing forces and surface topography.*

the topography's surface. M_r is the mass of the mobile platform, g is the acceleration of gravity (9.81 m/s^2), and $\ddot{x}$ is the linear acceleration of mobile platform.

Since there are two driving wheels (rear wheels), see Figure 1, and applying the superposition theory on every disturbing force (F_d) of Equation 15 yields the driving force produced by every actuator device independently from the other. For a single wheel, the driving force is given by:

$$f_d = f_i + f_w + f_f \tag{16}$$

with $f_i = \frac{M_r}{2}\ddot{x}_s$, $f_w = \frac{M_r}{2} g\sin(\beta)$

where: $\ddot{x}_s$ is the linear acceleration of a single driving wheel. The driving torques of a single actuator drive are:

$$T_d = T_i + T_w + T_f = r\,f_d = r\,f_i + r\,f_w + T_f \tag{17}$$

substituting for f_i, f_w ,and T_f in Equation 17 yields:

$$T_d = r^2\,\frac{M_r}{2}\ddot{\theta} + r\,\frac{M_r}{2} g\sin(\beta) + \xi\,\dot{\theta} \tag{18}$$

where: T_d is the disturbing torque of a single driving wheel, r is the wheel's radius, ξ is the viscous rolling friction coefficient between the wheel and the topography's surface, and ($\dot{\theta}$ = ω) and $\ddot{\theta}$ are the angular velocity and angular acceleration of the wheel, respectively.

Figure 8 presents a complete model in the form of block diagram of an armature controlled power actuator drive of a general mobile robot under the influence of disturbances and topography. The figure shows that changes in the topography inclination angle (β) is a disturbance introduced to the system. The needed controller should be robust, i.e. it should have a disturbance rejection. For the purpose of controller design, assume β = 0º and later on check the robustness of the controller, and substituting for ω(s) from the transfer function of the tachogenerator, Equation 14, yields the overall open loop transfer function of an armature control power actuator drive of a wheeled mobile robot, i.e. the transfer function from the armature input terminal voltage, $V_a(s)$ to the output terminal voltage of the tachogenerator U(s):

$$G_A(s) = \frac{U(s)}{V_a(s)} = \frac{2\,K\,K_m}{(r^2 M_r + 2\mu)L_a s^2 + \{(r^2 M_r + 2\mu)R_a + (\xi + 2J)L_a\}s + [(\xi + 2\,J)\,R_a + 2K_b K_m]} \tag{19}$$

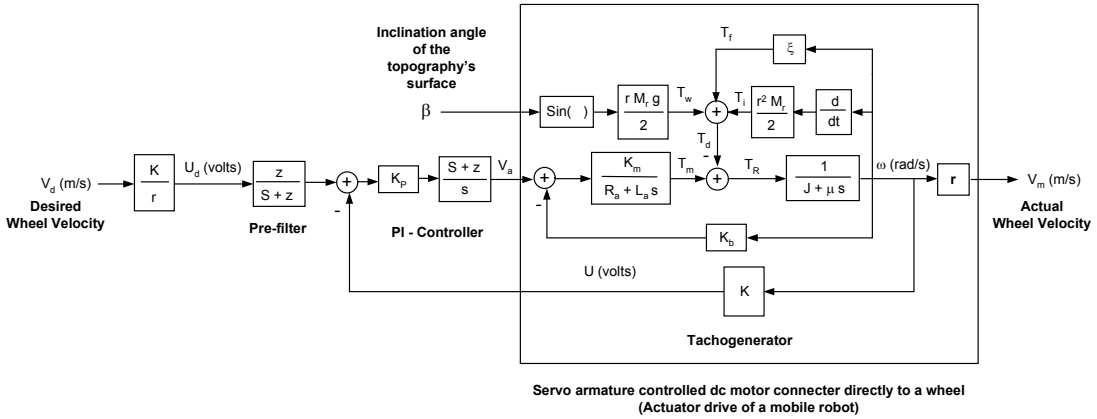

Figure 8. *Block diagram of an armature controlled power actuator drive of a general mobile robot.*

5. ANALOG CONTROL OF THE ACTUATOR DRIVES

A suitable controller for the actuator drives of wheeled mobile robots could be a *proportional-integral (PI) controller with deadbeat response*. Deadbeat response means the response that proceeds rapidly to the desired level and holds at that level with minimal overshoot, [6]. Deadbeat response has the following characteristics:

1- Zero steady state error.
2- Fast response, i.e. minimum rise time and settling time.
3- 0.1 % ≤ percent overshoot < 2 %.
4- Percent undershoot < 2 %.

The ± 2 % band at the desired level could be an acceptable range of variation from the desired response. The general form of a PI-controller is:

$$G_C(s) = K_P + \frac{K_I}{s} = K_P \frac{(s+z)}{s} \qquad (20)$$

Where: K_P is the proportional gain, K_I is the integrator gain, and $z = \frac{K_I}{K_P}$.

The closed-loop transfer function, T(s), of the actuator drive system becomes:

$$T(s) = \frac{K_F (s+z)}{s^3 + C_2 s^2 + C_1 s + C_0} \qquad (21)$$

with: $K_F = \frac{2KK_m K_P}{(r^2 M_r + 2\mu) L_a}$, $C_2 = \frac{R_a}{L_a} + \frac{(\xi + 2J)}{(r^2 M_r + 2\mu)}$,

$C_1 = \frac{(\xi + 2J)R_a + 2K_m(K_b + KK_P)}{(r^2 M_r + 2\mu)L_a}$,and

$C_0 = \frac{2KK_m K_I}{(r^2 M_r + 2\mu)L_a}$

The controller (compensator) $G_C(s)$ alters the roots of the characteristic equation of the closed-loop actuator drive system. The closed-loop transfer function, T(s), contains the zero of the PI-controller, $G_C(s)$. This zero will significantly affect the response of the closed-loop system, T(s), and should be eliminated while maintaining the gain (K_F) of the closed-loop system that can be achieved by a pre-filter. Thus, the requiring pre-filter is $G_P(s) = \frac{z}{s+z}$, and the overall transfer function, $T_A(s)$, of an armature controlled actuator drive system of a wheeled mobile robot becomes:

$$T_A(s) = \frac{z K_F}{s^3 + C_2 s^2 + C_1 s + C_0} \qquad (22)$$

To determine the coefficients (K_P, K_I, and z) that yield optimal deadbeat response, the transfer function $T_A(s)$ is compared with standard third order transfer function that is given by:

$$q(s) = \frac{\omega_n^3}{s^3 + \alpha\omega_n s^2 + \beta\omega_n^2 s + \omega_n^3} \qquad (23)$$

with α, β and ω_n are known coefficients of system with deadbeat response, see e.g. [6]. Comparing the characteristic equation of $T_A(s)$ with that of q(s) yields:

$C_2 = \alpha\omega_n$, $C_1 = \beta\omega_n^2$, and $C_0 = \omega_n^3$

$$\Rightarrow K_P = \frac{\{\beta\omega_n^2 (r^2 M_r + 2\mu) L_a\} - \{(\xi + 2J) R_a + 2K_m K_b\}}{2K_m K}$$

$$\Rightarrow K_I = \frac{\omega_n^3 (r^2 M_r + 2\mu) L_a}{2K_m K}, \quad \text{and}$$

$$z = \frac{K_I}{K_P} = \frac{\omega_n^3 (r^2 M_r + 2\mu) L_a}{\{\beta\omega_n^2 (r^2 M_r + 2\mu) L_a\} - \{(\xi + 2J) R_a + 2K_m K_b\}}$$

The required coefficients are: α = 1.9, β = 2.2 and $\omega_n T_s$ = 4.04, see e.g. [6]. If we select a settling time T_s (2 % criterion) of 0.05 seconds, then ω_n = 808 rad/ sec.

The same procedure can be followed for designing a PI-controller with pre-filter for a field control actuator drive of mobile robot.

6. CONCLUSIONS

For the purpose of simulation of a real armature control power actuator drive of a real wheeled mobile platform, a global simulation model is constructed in Matlab and Simulink software. Figure 8 presents block diagram of the simulation model and Table 1 presents the needed, and used physical parameters of the considered mobile platform. Figure 9 presents step responses for the actuator drive of the mobile robot. The results are repeatable for different surface topography inclination angles (β = -30°, -15°, 0°, 15°, and 30°) that prove the robustness of the designed optimal PI-controller. Figure 10 simulates point-to-point motion control of the mobile platform showing the path of the robot. At the initial position (1,1) the robot is directed toward the left hand side, so it has to make a rotation in order to direct itself toward the target position (5,5).

The results show that the models of the actuator drives of the mobile robot can be used to simulate any mobile robot. The designed PI-control with pre-filter is optimal and robust. The controller gains K_P, K_I and z depend on the physical parameters of the actuator drives, and the topography acts as a disturbance on the controller, that make the controller suitable for controlling any armature control actuator drive of mobile platforms.

The designed simulation model can be used for simulating tasks of mobile robots such as point-to-point motion control, path following, and obstacle avoidance.

Table 1: *Physical parameters of a wheeled mobile platform .*

Name	Symbol	Value	Units
DC motor torque constant	K_m	4.1×10^{-2}	N.m/ A
Motor back e.m.f. constant	K_b	0.041	V.sec/ rad
Armature resistance	R_a	1.9	Ω
Armature inductance	L_a	1.0×10^{-3}	H
Armature time constant	τ_a	0.53×10^{-3}	Sec
Motor rotor moment of inertia	J_{MR}	0.0214×10^{-3}	Kg/ m^2
Mechanical time constant	τ_R	24.5×10^{-3}	Sec
Wheel radius	r	40×10^{-3}	m
Wheel thickness	t	32×10^{-3}	m
Wheel moment of inertia	J_W	3.8486×10^{-3}	Kg/ m^2
Rotor and wheel moment of inertia	J	3.8700×10^{-3}	Kg/ m^2
Bearing's viscous friction coefficient	μ	0.16	N.m.Sec
Viscous friction coefficient between wheel and ground	ξ	0.08	N.m.Sec
Tachogenerator voltage constant	K	31×10^{-3}	V.Sec/ rad
Tachogenerator resistance	R	12	Ω
Tachogenerator maximum continuous speed	ω_{max}	314	Rad/ Sec
Mobile platform total mass	M_r	3.0	Kg

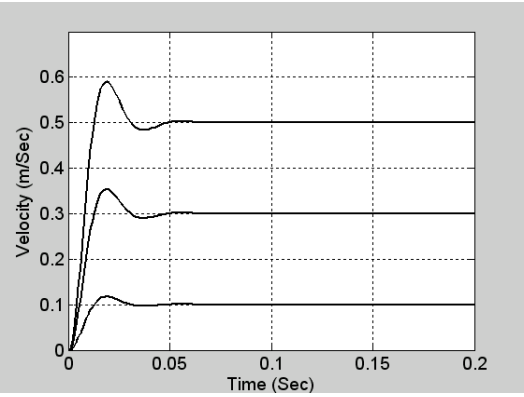

Figure 9. *Step responses for the actuator drive of the simulated mobile robot.*

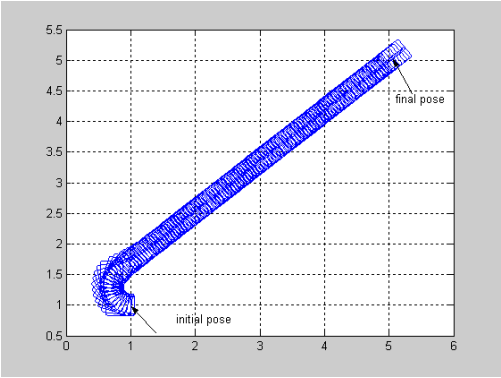

Figure 10. *Simulation results of point-to-point motion control of the mobile platform.*

7. REFERENCES

[1] Dudek Gregory, and Michael Jenkin, *Computational principles of mobile robotics*. Cambridge university press, 2000.

[2] Egerstedt, M., X. Hu and A. Stotsky. "Control of mobile platforms using a virtual vehicle approach," *IEEE Trans. on automatic control*, *Vol. 46, No. aa, 2001, p1777-1782.*

[3] Doh-Hyum Kim and Jun-Ho Oh. "Globally asymptotically stable tracking control of mobile robots," *Proceedings of the IEEE International conference on control applications*, 1297-1301, Trieste, Italy, 1-4 September 1998.

[4] Zavlangas, Panagiotis G., Spyros G. Tzafestas, and K. Althoefer. "Fuzzy obstacle avoidance and navigation for omni directional mobile robots," *ESIT 2000*, 375-382, Aachen, Germany, 14-15 Sep. 2000.

[5] Amirouche, Farid, *Principles of Computer-Aided Design and Manufacturing*, Second Edition, Pearson Prentice Hall, New Jersey,2004.

[6] Richard C. Dorf and Robert H. Bishop. *Modern Control Systems*. Ninth Edition, Prentice-Hall Inc., New Jersey, 2001.

[7] Bentley, John P., *Principles of Measurement Systems*. Third Edition, Prentice Hall, United Kingdom, 1995.